EurJOC
European Journal of Organic Chemistry

A Journal of
ChemPubSoc Europe

Accepted Article

Title: Metal-free photocatalytic reductive dehalogenation using visible-light. A time-resolved mechanistic study

Authors: Rebeca Martinez-Haya, Miguel A Miranda, and Maria Luisa Marin

To be cited as: *Eur. J. Org. Chem.* 10.1002/ejoc.201601494

Link to VoR: http://dx.doi.org/10.1002/ejoc.201601494

Supported by
ACES Asian Chemical Editorial Society

WILEY-VCH

10.1002/ejoc.201601494

WILEY-VCH

Metal-free photocatalytic reductive dehalogenation using visible-light. A time-resolved mechanistic study

Rebeca Martinez-Haya,[a] Miguel A. Miranda[a] and M. Luisa Marin*[a]

Abstract: Reductive dehalogenation of organic bromides has been achieved in the presence of riboflavin (RF) as the photocatalyst under visible light irradiation. Specifically, benzyl bromide (**2**) and α-bromoacetophenone (**3**) were quantitatively converted into toluene and acetophenone, respectively, using amines as electron donors and *i*-PrOH as H-donor, while bromobenzene (**1**) remained unreacted. The thermodynamics of the reduction reaction from the radical anion of RF was evaluated using the redox potentials of the involved species: while it is not expected for bromobenzene (**1**), is thermodynamically exergonic for **2** and **3**. The viability of the different competing processes in the time scale of the corresponding singlet and triplet RF excited states (^{1}RF* and ^{3}RF*), was analyzed by time-resolved techniques. Quenching of ^{1}RF* by amines was very efficient, and the comparison of the transient absorption spectrum recorded in the absence and in the presence of amines acted as an additional confirmation of the efficient redox process from ^{1}RF*. Moreover, quenching of $RF^{\cdot-}$ was observed for bromides **2** and **3**, while **1** did not produce any change. Thus, deeper understanding of the overall mechanism of a photocatalytic reductive reaction has been achieved, and the key role of the radical anion of the photocatalyst has been demonstrated.

Introduction

In recent years, increasing attention has focused in photoredox catalysis using preferentially visible light. As a result of this effort, myriads of different applications of transition-metal based or the alternative metal-free photocatalysts, typically organic dyes, have been developed.[1]

Riboflavin (RF) is a natural dye present in waters of rivers, lakes and seas, responsible for the redox activity of cofactors flavin mononucleotide (FMN) and flavin adenine dinucleotide (FAD). It has a three-ring isoalloxazine chemical structure, a 7,8-dimethyl substitution and a ribotyl chain at the N 10 position (Figure 1). Its characteristic visible absorption spectrum exhibits two defined bands peaking ca. 450 and 350-375 nm, with high molar absorption coefficients. For this reason, RF has been considered as the most likely candidate to explain "natural" photodegradation of pollutants in the environment.[2] The photophysical properties of RF have been studied in detail; briefly, RF exhibits in aqueous solution a moderate fluorescence (λ_{max} = 510 nm) with a quantum yield of Φ_F = 0.26 (which increases up to 0.47 in CH_3CN), and an intersystem crossing quantum yield of Φ_{ISC} = 0.70. Furthermore, RF is able to sensitize generation of singlet oxygen from its triplet excited state with Φ_Δ = 0.47.[2] The RF singlet and triplet energies are 2.48 eV and 2.17 eV, respectively. Although the redox potential of RF depends on the solvent, values ranging between -0.80 V and -0.45 V have been reported.[3]

The capability of RF as a metal-free photocatalyst for water remediation, more specifically to promote photooxidation of phenolic or *N*-heteroaromatic pollutants upon solar irradiation, has been extensively reported.[4] Mechanistic studies, based on time-resolved techniques, have demonstrated that most of the pollutants are able to quench the singlet and/or the triplet excited states of RF, giving rise to the corresponding pollutant radical cations along with the characteristic $RF^{\cdot-}$, which shows a transient absorption spectrum with an intense maximum at 380 nm and a broad and less intense maximum in the 500-600 nm region.[4a, 5] Further oxidation has been attributed, in many cases, to the reactivity of the radical cations with superoxide anion, which results from the electron transfer process from $RF^{\cdot-}$ to O_2. More recently, RF or related flavin derivatives have also found applications as visible-light redox photocatalysts to produce different transformations with synthetic purposes, such as aerobic photooxidation of sulfides,[6] oxidative chlorination of arenes[7] or selective removal of benzylic protecting groups,[8] among others. However, no attention has been paid to the potential of RF as a reductant in either water remediation or organic synthesis.

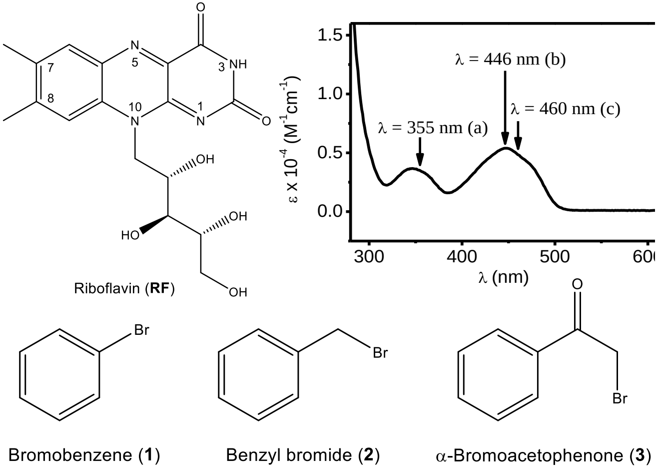

Figure 1. Chemical structure and absorption spectrum of Riboflavin (RF) in dimethylformamide (top); excitation wavelengths used for: (a) laser-flash photolysis; (b) steady-state emission and (c) time-resolved emission experiments; chemical structures of selected organic bromides (bottom).

---

[a] R. Martinez-Haya, M.A. Miranda and M.L. Marin
Instituto de Tecnología Química, Universitat Politècnica de València-Consejo Superior de Investigaciones Científicas,
Avenida de los Naranjos s/n, 46022 Valencia, Spain
E-mail: marmarin@qim.upv.es

Supporting information for this article is given via a link at the end of the document.

Reductive dehalogenation procedures that are of wide application in many different synthetic contexts have also been optimized using visible-light photocatalysts such as $Ru(bpy)_3Cl_2$;[9] however, the improvement of these reductive processes still remains a challenge for synthetic chemists.

Although a deeper mechanistic understanding of the underlying processes could help to broaden the substrate scope of the photocatalyzed organic reactions, most of the recent publications lack a kinetic study of the involved excited states. However, postulated reaction mechanisms should be the result of investigating on the photophysical properties of the employed photocatalysts for determining the kinetic parameters of the competitive pathways they undergo in the presence of different substrates.[4a, 10]

In this context, the goal of the present work is to gain understanding on the overall reactions mechanisms by analyzing the thermodynamic and the kinetic feasibility of all the competing pathways of the photocatalyzed redox processes. For this purpose, the kinetic constants of every step will be determined using fast kinetic techniques, to postulate a plausible mechanism based on the experimentally obtained results. Such a protocol will be applied to investigate on the capability of RF as a metal-free photocatalyst to produce reductive dehalogenation of different bromo-derivatives, upon irradiation using visible light, and in the presence of amines and isopropanol as e^- and H-donors, respectively. Specifically, bromides such as bromobenzene (**1**), benzyl bromide (**2**) and α-bromoacetophenone (**3**) have been selected (Figure 1).

Results and Discussion

Photocatalyzed reactions

Initially, **3** was selected to optimize the experimental conditions of the photodegradation reaction. We tested 1,4-diazabicyclo[2.2.2]octane (DABCO, 2 eq) as the e^- donor and *i*-PrOH (2 eq) as the H-donor. Irradiations were performed in DMF:H_2O, DMSO:H_2O and CH_3CN:H_2O, in the presence of RF (2.5 mol %) under inert atmosphere, and using two LEDs (λ_{em} = 460 nm, 20 W each). Final conversion (up to 18 h irradiation) was low, mainly due to solubility problems. Change to diisopropyl amine (DIPA) in DMF:H_2O ensured good solubility and allowed increasing the amount of amine up to 5 eq. Under these conditions, 100% conversion to acetophenone was observed upon 12 h irradiation. Although it has been described that RF tends to form aggregates due to H-bonding and $\pi\pi$ interactions, that can be decreased in the presence of water,[6] the use of DMSO as a solvent in the absence of water also resulted in 100% conversion. Reducing the equivalents of amine and *i*-PrOH to 1 eq each, decreased the rate of conversion, but still 100% was obtained upon 18 h. When dehalogenation was conducted under air, observed conversion was low and other side-products were found in the HPLC analysis, maybe due to the formation of $O_2^{\cdot-}$ that caused photodegradation of RF among other side processes. Control experiments carried out in the absence of light or in the absence of RF resulted only in 10% conversion; therefore the selected reaction conditions are shown in Scheme 1. Next, we tested the dehalogenation of **2** under the same conditions, and again 100% conversion was achieved. Due to the volatility of the expected toluene, the final compound was difficult to detect; however, increasing the initial benzyl bromide concentration from 6.2 x10^{-2} M to 2.5 x10^{-1} M allowed monitoring a clean quantitative conversion of **2** into toluene. Same reaction conditions as those used for **2** were applied to bromobenzene (**1**); nevertheless it remained unreacted even at longer irradiation times.

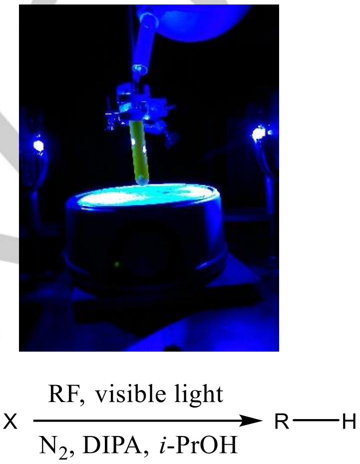

$$R{-}X \xrightarrow[N_2,\ DIPA,\ i\text{-}PrOH]{RF,\ visible\ light} R{-}H$$

Scheme 1. Representative set-up to perform the reductive dehalogenation of bromides using RF as metal-free photocatalyst and blue LEDs.

Thermodynamic feasibility of the involved processes

To postulate a plausible reaction mechanism explaining reductive dehalogenation of bromides we analyzed the thermodynamic feasibility of all the potentially involved processes (Scheme 2).

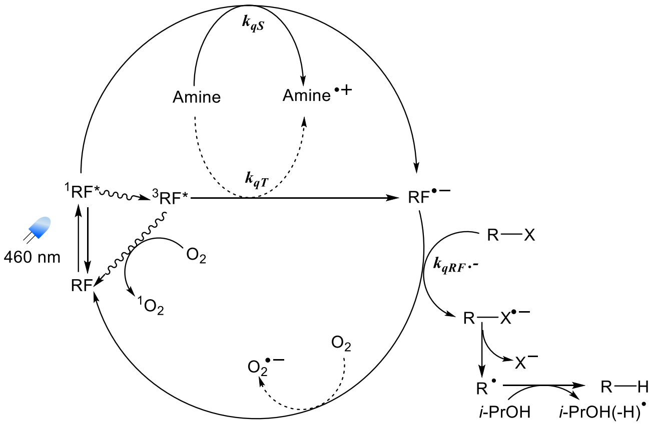

Scheme 2. Postulated reaction mechanism.

Quenching of the excited states of a photocatalyst could, in principle, be due to two different mechanisms: energy transfer or electron transfer. By comparing the UV-visible spectra of the photocatalyst and the bromides (See Figure 1 and SI), while RF absorbs up to 500 nm, all the studied bromides absorb at much shorter wavelength, below 300 nm for **1** and **2**, and below 400 nm in the case of **3**. Therefore, one can anticipate much more energetic excited states in the case of the bromides than in the case of RF (singlet and triplet energies for RF are 2.48 eV and 2.17 eV, respectively).[3b] As a result, the energy transfer from RF is thermodynamically disfavored in all cases and can be safely ruled out. According to the proposed mechanism, reduction of the bromides should occur from the $RF^{\cdot-}$, that would be generated from the singlet and/or triplet excited states of RF in the presence of e^- donors such as DABCO, DIPA, *N,N'*-dimethylaniline (DMA) or triethylamine (TEA). Thus, we studied the feasibility of the photoinduced electron transfer from the different amines to the excited states of RF using the Gibbs energy of photoinduced electron transfer equation (formerly known as Rehm-Weller equation):[11]

$$\Delta G_{et}^{o}(eV) = -(E_{red}^{o}(RF/RF^{\cdot-}) - E_{red}^{o}(D^{\cdot+}/D)) - E(RF^{*}) + \Delta E_{Coulombic}$$

The redox potential of RF has been reported as $E_{red}^{o}(RF/RF^{\cdot-})$ = -0.80 V (*vs.* SCE) in DMSO (see above). The reported redox potential values for the oxidation of different amines are shown on Table 1. By applying the Gibbs energy of photoinduced electron transfer equation we can conclude that oxidation of the amines from the singlet or the triplet excited state of RF is in every case exergonic.

Then, once the radical anion of RF is obtained, next step would be the reduction of the bromides. The thermodynamics of these processes could be evaluated using the redox potentials of the involved species by applying the "thermal" free Gibbs energy equation:

$$\Delta G^{o}(eV) = -(E_{red}^{o}(C-Br/C-Br^{\cdot-}) - E_{red}^{o}(RF/RF^{\cdot-}))$$

Table 1. Thermodynamic redox potentials and determined rate constants for the quenching of excited states of RF or $RF^{\cdot-}$ by amines or bromides selected in the photocatalytic dehalogenation reactions.

	$E(D^{\cdot+}/D)$ [a]	$E(A/A^{\cdot-})$[a]	k_{qS} [b]	k_{qT} [b]	$k_{qRF^{\cdot-}}$ [b]
DABCO	+0.56[12]	-	4.5 $\times10^{9}$	N.D.	-
DIPA	+1.31[3b]	-	1.6 $\times10^{9}$	N.D.	-
DMA	+0.81[12]	-	5.3 $\times10^{9}$	N.D.	-
TEA	+0.96[12]	-	2.9 $\times10^{9}$	N.D.	-
1	-	-1.56[13]	-	-	$< 10^{6}$
2	-	-0.57[13]	-	-	9.1×10^{7}
3	-	-0.49[14]	-	-	1.7×10^{8}
O_2	-	-0.33[15]	-	9.0×10^{8}[4b]	1.4×10^{8}[4b]

[a] in V *vs* SCE. [b] $M^{-1}s^{-1}$. N.D.: not determined.

Using this equation the resulting ΔG^{o} are: +0.76 eV; -0.23 eV and -0.31 eV, for bromides **1**, **2** and **3**, respectively. Thus, while reduction of bromobenzene (**1**) is not expected from the $RF^{\cdot-}$, reduction of **2** and **3** is thermodynamically exergonic.

Kinetic viability of the involved processes

Having analyzed the thermodynamics, the following step was to determine the viability of the different competing processes in the time scale of the corresponding RF excited states. First, the participation of the singlet excited state was investigated by means of steady-state and time-resolved fluorescence and then laser flash photolysis was used to monitor the dynamics of the triplet excited state as well as the radical anion.

Steady-state and time-resolved emission results

Quenching of the known $^1RF^*$ fluorescence by amines was performed in aerated DMF. In all cases it proceeded without changes of the emission spectral shape; likewise, no changes were found in the absorption spectrum of RF, thus precluding formation of ground state complexes. Conversely, an efficient emission quenching was observed in all cases (see Figure 2 top for the case of DIPA and SI for the rest of them). Moreover, time-resolved emission showed a very efficient quenching (Figure 2 middle and SI) upon addition of DABCO, DIPA, DMA or TEA, in agreement with the expectations taking into account the redox potential of RF and those of the employed amines (see Table 1).[3b] The corresponding quenching constants were determined from the Stern-Volmer relationships (Figure 2 bottom and SI). The obtained data (see Table 1) confirmed the dynamic participation of $^1RF^*$ in the electron transfer process, with values close to the diffusion limit.[12] On the other hand, control experiments showed that singlet lifetime of $^1RF^*$ remained unchanged upon addition of bromides **1**-**3**, up to 5 x 10^{-2} M concentration (see SI), indicating that $^1RF^*$ is unreactive in the presence of the bromides, as expected from their redox potentials.

Laser flash photolysis experiments

Involvement of $^3RF^*$ was investigated by laser flash photolysis (LFP) experiments. Upon excitation of a deaerated solution of RF (4 x 10^{-5} M) in DMF, the typical band with a maximum centered at 380 and a huge band between 500 and 700 nm, corresponding to the already described triplet excited state ($^3RF^*$) were obtained (see Figure 3 and SI).[4a] Conversely, when the spectrum was recorded in the presence of one of the above mentioned amines a completely different signal appeared, with a much more intense maximum at 380 nm (assigned to $RF^{\cdot-}$, based on literature data)[4a 5] and a less intense wide band between 500 and 650 nm (see Figure 3 for the case of DABCO). The comparison of the transient absorption spectrum recorded in the absence and in the presence of amine acted as an additional confirmation of the efficient redox process between the $^1RF^*$ and the amines. Furthermore, the e^- transfer from the amines to the $^3RF^*$, as postulated in Scheme 2, was difficult to monitor accurately due to the efficient quenching of $^1RF^*$. Thus when traces at 620 nm (basically $^3RF^*$) were recorded in the absence and in the presence of amine a huge decrease in the transient absorbance immediately after the laser shot was observed but a decrease in the triplet lifetime was not clear (Figure 4). Nevertheless, when monitoring the trace at 380 nm in the presence of the amine, a small but significant contribution from the $^3RF^*$ to $RF^{\cdot-}$ conversion was observed. Control experiments performed in the presence of the bromides **1**-**3** showed no direct reaction from the $^3RF^*$ (see SI).

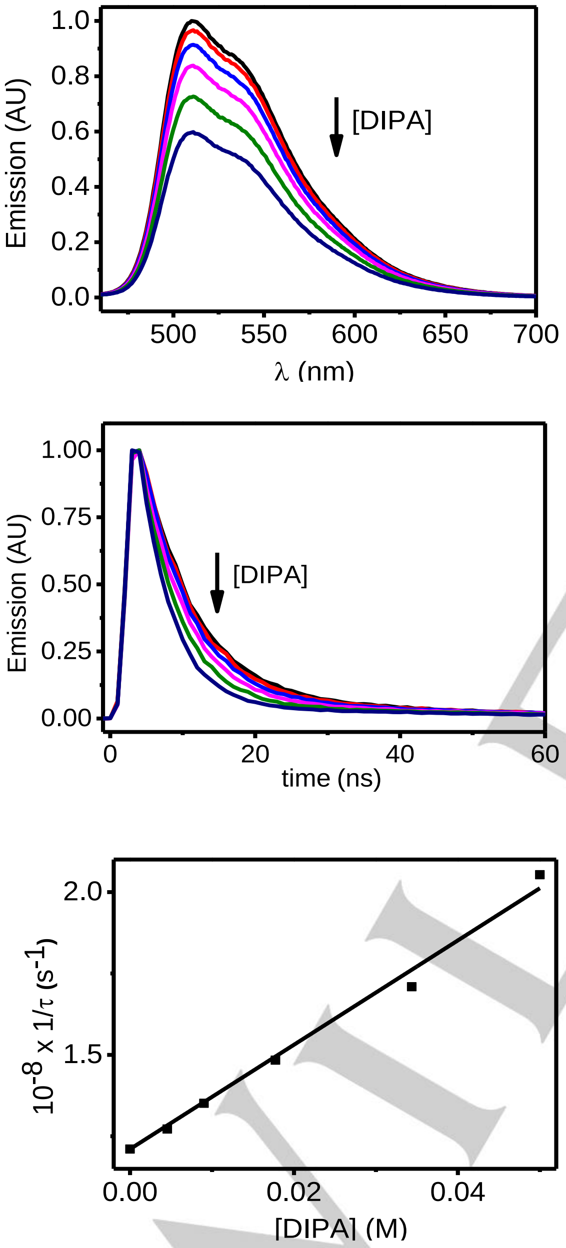

Figure 2. Top: Steady-state (λ_{exc}= 446 nm) emission behavior of RF and middle: changes in the singlet lifetime of RF (λ_{exc}= 460 nm), in the presence of increasing concentrations of DIPA in aerated dimethylformamide. Bottom: Stern-Volmer plot obtained from the time-resolved experiments.

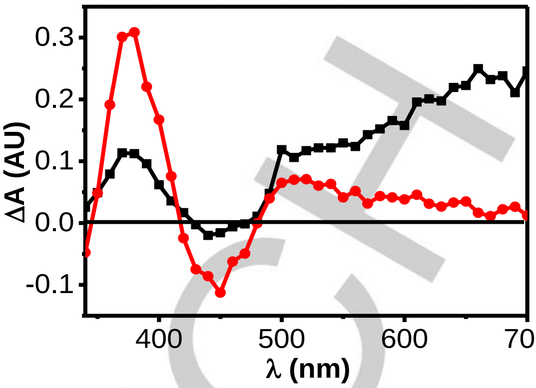

Figure 3. Transient absorption spectra obtained upon laser flash excitation of RF in deaerated DMF (λ_{exc} = 355 nm) recorded 2 μs after the laser pulse in the absence (black) and in the presence of DABCO 5.4 x 10^{-2} M (red).

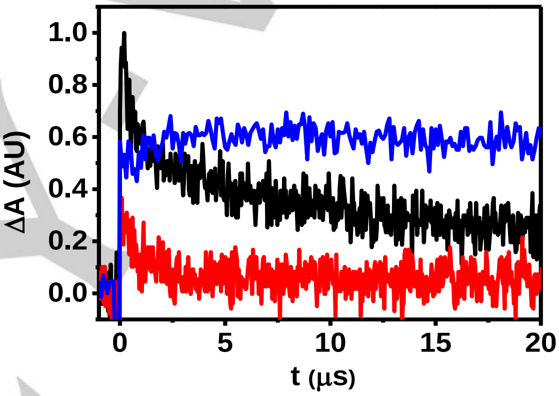

Figure 4. Traces recorded upon laser flash photolysis excitation of RF (4 x 10^{-5} M) in deaerated DMF (λ_{exc} = 355 nm). Black: $^3RF^*$ monitored at 620 nm; red: remaining $^3RF^*$ monitored at 620 nm in the presence of DABCO 5.4 x 10^{-2} M; blue: growth of $RF^{\cdot-}$ monitored at 380 nm.

Next step was to test the quenching of the $RF^{\cdot-}$ by the bromides **1**-**3**. For this purpose, a deaerated solution of RF (4 x 10^{-5} M) and DABCO (5.4 x 10^{-2} M) in DMF was subjected to LFP excitation and the evolution of the radical anion was monitored in the presence of increasing concentrations of the bromides (see Figure 5). As anticipated from the thermodynamic study, while bromides **2** and **3** quenched the $RF^{\cdot-}$, bromide **1** did not produce any change. From the Stern-Volmer analysis values of 9.1 x 10^7 and 1.7 x 10^8 $M^{-1}s^{-1}$ were determined for **2** and **3**, respectively (Figure 5 and Table 1).

The limiting quantum yield of $RF^{\cdot-}$ formation due to the quenching of $^1RF^*$ or $^3RF^*$ can be evaluated from the following equations:

$$\Phi_{RF^{\cdot-}}(from\ ^1RF^*) = \frac{k_{qS}[Amine]}{\frac{\Phi_F}{\tau_S}+\frac{\Phi_{ISC}}{\tau_S}+k_{qS}[Amine]} \qquad \text{(eq 1)}$$

$$\Phi_{RF^{\cdot-}}(from\ ^3RF^*) = \frac{\frac{\Phi_{ISC}}{\tau_S}}{\frac{\Phi_F}{\tau_S}+\frac{\Phi_{ISC}}{\tau_S}+k_{qS}[Amine]} \times \frac{k_{qT}[Amine]}{\frac{1}{\tau_T}+k_{qT}[Amine]}$$

(eq 2)

10.1002/ejoc.201601494

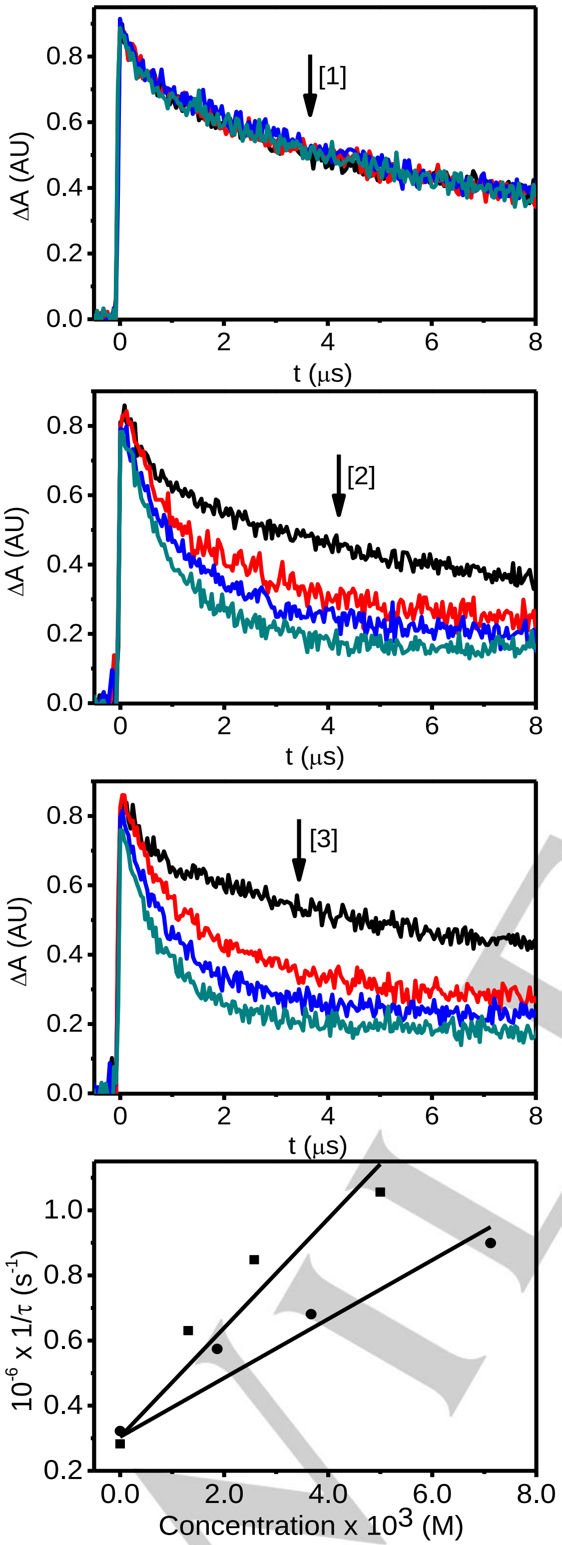

Figure 5. Traces corresponding to $RF^{\bullet -}$ monitored at 380 nm upon laser flash photolysis excitation of RF (4 x 10^{-5} M) and DABCO (xx mM) in deaerated DMF (λ_{exc} = 355 nm) in the presence of increasing concentratios of bromides **1**-**3**. Bottom: Stern-Volmer plot corresponding to the quenching of $RF^{\bullet -}$ by bromides **2** (circles) and **3** (squares).

Taking the reported $\Phi_F = 0.26$ and $\Phi_{ISC} = 0.70$, the determined value of τ_S = 8.3 ns, an average experimental value of 3 x 10^9 $M^{-1}s^{-1}$ for the quenching of the singlet by amines in our hands, and a value of 0.3 M for the concentration of the amines under the experimental conditions, the quantum yield for the $\Phi_{RF^{\bullet -}}$ from $^1RF^*$ (according to eq. 1) is *ca.* 0.90. This means that quenching from the singlet is almost quantitative, supporting the postulated mechanism (Scheme 2). Quenching of $RF^{\bullet -}$ by bromides **2** and **3** is of the same order of magnitude as quenching by O_2 to produce superoxide anion. Although concentration of O_2 in aerated DMSO would be much lower than the concentration of the bromides, still formation of $O_2^{\bullet -}$ could be responsible for the degradation of RF (only used at 2.5 mol %) and thus for the low observed yields when reactions were performed under air.

Conclusions

Time-resolved techniques have proven useful to analyze the kinetic feasibility of the thermodynamically allowed competing pathways of the photocatalyzed redox processes. Firstly, quenching of the singlet excited state of riboflavin ($^1RF^*$) by amines proceeds with kinetic constant values close to diffusion and is accompanied by formation of the radical anion ($RF^{\bullet -}$). Secondly, quenching of $RF^{\bullet -}$ by the organic bromides gives rate constant values according to the thermodynamic estimations for the thermal redox process; therefore demonstrating the key role of this intermediate. Thus, deeper understanding of the overall mechanism of photocatalytic reductive reaction has been achieved, and the key role of the radical anion of the photocatalyst has been demonstrated.

Experimental Section

Chemicals

Riboflavin (RF), 1,4-diazabicyclo[2.2.2]octane (DABCO), diisopropyl amine (DIPA), *N,N'*-dimethylaniline (DMA), triethylamine (TEA), bromobenzene (**1**), benzyl bromide (**2**), α-bromoacetophenone (**3**) and 1,3,5-trimethylbenzene were obtained from Aldrich. Dimethylformamide (DMF) 99% purity was from Accross, CH_3CN was of HPLC quality from Scharlau and anhydrous dimethylsulfoxide (DMSO) was from Aldrich. Milli-Q grade water was used for the HPLC analyses.

Photocatalytic reductive dehalogenation

Photocatalytic reactions were performed at 0.5 mmol scale in the case of **3** or 2 mmol scale for **1** and **2**. Typical procedure is as follows: DMSO solutions of 8 mL containing a mixture of one of the bromides and RF (2.5 mol %) were irradiated using two LEDs centered at 460 nm, under N_2 atmosphere, in the presence of DIPA (2-5 eq) and *i*-PrOH (2-5 eq) in Pyrex tubes. To monitor the reactions, aliquots were taken and injected into the HPLC (Waters 600 C chromatograph equipped with a Waters 600 Pump and Controller, a Waters in-Line degasser AF and a Waters 996 Photodiode Array Detector). A Teknokroma C18 Mediterranea Sea (25 × 0.46 mm and 5 μm particle size) analytical column was used as stationary phase, and a mixture of acetonitrile/water was used as eluent working in isocratic mode (70% acetonitrile) at a flow rate of 1.5 mL min^{-1}. 1,3,5-Trimethylbenzene (10 μL of a 0.2 M solution) was added as internal standard to every aliquot (5 μL) before injection. The chromatograms were analyzed at 250 or 275 nm. Starting materials and final compounds were identified by comparison to commercial standards.

Photophysical instrumentation

A Shimadzu UV-2101PC spectrophotometer was employed to perform the UV/Vis absorption spectra. Steady-state and time-resolved fluorescence experiments were carried out on a Photon Technology International (PTI) LPS-220B spectrofluorometer and on a EasyLife V spectrofluorometer from OBB, respectively. In the case of time-resolved fluorescence, the apparatus was equipped with a diode LED (λ_{exc} = 460 nm) excitation source; residual excitation signal was filtered in emission by using a cut-off filter (50% transmission at 475 nm). A pulsed Nd: YAG SL404G-10 Spectron Laser Systems at the excitation wavelength of 355 nm was employed to carry out the laser flash photolysis (LFP) experiments. The energy of the single pulses (~10 ns duration) was lower than 30 mJ $pulse^{-1}$. The laser flash photolysis system is formed by the pulsed laser, a pulsed Lo255 Oriel Xenon lamp, a 77200 Oriel monochromator, an Oriel photomultiplier tube (PMT) housing, a 70705 PMT power supply and a TDS-640A Tektronix oscilloscope. Photophysical measurements were run at room temperature under nitrogen using quartz cells of 1 cm optical path length.

For the steady-state and time-resolved fluorescence experiments, aerated DMF solutions of RF (absorbance lower than 0.15 at λ_{exc} = 446 or 460 nm, respectively) were treated with increasing concentrations of amine or bromoderivative (up to 5 x 10^{-2} M). Transient absorption experiments were performed on deaerated solutions of RF in DMF (4 x 10^{-5} M).

Acknowledgements

R. Martinez-Haya acknowledges generous support from Spanish Government (Grant SEV-2012-0267). We also thank support from Generalitat Valenciana (Prometeo Program) and VLC/Campus.

Keywords: electron transfer • photophysics • reactive intermediates • redox chemistry • time-resolved spectroscopy

[1] a) G. J. Kavarnos, N. J. Turro, *Chem. Rev.* **1986**, *86*, 401-449; b) M. Fagnoni, D. Dondi, D. Ravelli, A. Albini, *Chem. Rev.* **2007**, *107*, 2725-2756; c) J. Xuan, W.-J. Xiao, *Angew. Chem. Int. Ed.* **2012**, *51*, 6828-6838; d) D. Ravelli, M. Fagnoni, A. Albini, *Chem. Soc. Rev.* **2013**, *42*, 97-113; e) S. Fukuzumi, K. Ohkubo, *Chem. Sci.* **2013**, *4*, 561-574; f) S. P. Pitre, C. D. McTiernan, J. C. Scaiano, *Acc. Chem. Res.* **2016**, *49*, 1320-1330; g) D. Staveness, I. Bosque, C. R. J. Stephenson, *Acc. Chem. Res.* **2016**, *49*, 2295-2306; h) K. L. Skubi, T. R. Blum, T. P. Yoon, *Chem. Rev.* **2016**, *116*, 10035-10074; i) M. H. Shaw, J. Twilton, D. W. C. MacMillan, *J. Org. Chem.* **2016**, *81*, 6898-6926; j) N. A. Romero, D. A. Nicewicz, *Chem. Rev.* **2016**, *116*, 10075-10166.

[2] P. F. Heelis, *Chem. Soc. Rev.* **1982**, *11*, 15-39.

[3] a) C. Lu, W. Lin, W. Wang, Z. Han, S. Yao, N. Lin, *Phys. Chem. Chem. Phys.* **2000**, *2*, 329-334; b) G. Porcal, S. G. Bertolotti, C. M. Previtali, M. V. Encinas, *Phys. Chem. Chem. Phys.* **2003**, *5*, 4123-4128; c) A. Masek, E. Chrzescijanska, M. Zaborski, M. Maciejewska, *C. R. Chimie* **2012**, *15*, 524-529; d) S. L. J. Tan, R. D. Webster, *J. Am. Chem. Soc.* **2012**, *134*, 5954-5964; e) W. Chen, J.-J. Chen, R. Lu, C. Qian, W.-W. Li, H.-Q. Yu, *Bioelectrochemistry* **2014**, *98*, 103-108.

[4] a) M. L. Marin, L. Santos-Juanes, A. Arques, A. M. Amat, M. A. Miranda, *Chem. Rev.* **2012**, *112*, 1710-1750; b) A. Pajares, J. Gianotti, G. Stettler, S. Bertolotti, S. Criado, A. Posadaz, F. Amat-Guerri, N. A. Garcia, *J. Photochem. Photobiol., A* **2001**, *139*, 199-204; c) W. Massad, S. Criado, S. Bertolotti, A. Pajares, J. Gianotti, J. P. Escalada, F. Amat-Guerri, N. A. Garcia, *Chemosphere* **2004**, *57*, 455-461; d) E. Haggi, S. Bertolotti, N. A. Garcia, *Chemosphere* **2004**, *55*, 1501-1507; e) N. A. García, F. Amat-Guerri, *Chemosphere* **2005**, *59*, 1067-1082; f) Y. Barbieri, W. A. Massad, D. J. Diaz, J. Sanz, F. Amat-Guerri, N. A. Garcia, *Chemosphere* **2008**, *73*, 564-571; g) J. P. Escalada, A. Pajares, J. Gianotti, W. A. Massad, S. Bertolotti, F. Amat-Guerri, N. A. Garcia, *Chemosphere* **2006**, *65*, 237-244; h) M. Diaz, M. Luiz, P. Alegretti, J. Furlong, F. Amat-Guerri, W. Massad, S. Criado, N. A. Garcia, *J. Photochem. Photobiol., A* **2009**, *202*, 221-227; i) A. Pajares, M. Bregliani, M. P. Montana, S. Criado, W. Massad, J. Gianotti, I. Gutierrez, N. A. Garcia, *J. Photochem. Photobiol., A* **2010**, *209*, 89-94.

[5] S. G. Bertolotti, C. M. Previtali, A. M. Rufs, M. V. Encinas, *Macromolecules* **1999**, *32*, 2920-2924.

[6] T. Nevesely, E. Svobodova, J. Chudoba, M. Sikorski, R. Cibulka, *Adv. Synth. Catal.* **2016**, *358*, 1654-1663.

[7] T. Hering, B. Muhldorf, R. Wolf, B. Konig, *Angew. Chem., Int. Ed.* **2016**, *55*, 5342-5345.

[8] R. Lechner, B. Konig, *Synthesis-Stuttgart* **2010**, 1712-1718.

[9] a) J. M. R. Narayanam, J. W. Tucker, C. R. J. Stephenson, *J. Am. Chem. Soc.* **2009**, *131*, 8756-8757; b) L. Furst, B. S. Matsuura, J. M. R. Narayanam, J. W. Tucker, C. R. J. Stephenson, *Org. Lett.* **2010**, *12*, 3104-3107; c) J. J. Devery, J. D. Nguyen, C. Dai, C. R. J. Stephenson, *ACS Catal.* **2016**, *6*, 5962-5967; d) I. Ghosh, T. Ghosh, J. I. Bardagi, B. König, *Science* **2014**, *346*, 725; e) I. Ghosh, L. Marzo, A. Das, R. Shaikh, B. König, *Acc. Chem. Res.* **2016**, *49*, 1566-1577; f) J. D. Nguyen, E. M. D'Amato, J. M. R. Narayanam, C. R. J. Stephenson, *Nat. Chem.* **2012**, *4*, 854-859; g) E. H. Discekici, N. J. Treat, S. O. Poelma, K. M. Mattson, Z. M. Hudson, Y. Luo, C. J. Hawker, J. R. de Alaniz, *Chem. Commun.* **2015**, *51*, 11705-11708; h) I. Ghosh, B. König, *Angew. Chem. Int. Ed.* **2016**, *55*, 7676-7679; i) L. Zeng, T. Liu, C. He, D. Shi, F. Zhang, C. Duan, *J. Am. Chem. Soc.* **2016**, *138*, 3958-3961; j) M. Haring, R. Perez-Ruiz, A. Jacobi von Wangelin, D. D. Diaz, *Chem. Commun.* **2015**, *51*, 16848-16851; k) M. Majek, U. Faltermeier, B. Dick, R. Pérez-Ruiz, A. Jacobi von Wangelin, *Chem. Eur. J.* **2015**, *21*, 15496-15501.

[10] a) G. M. Rodriguez-Muñiz, J. Gomis, A. Arques, A. M. Amat, M. L. Marin, M. A. Miranda, *Photochem. Photobiol.* **2014**, *90*, 1467-1469; b) R. Martinez-Haya, J. Gomis, A. Arques, M. L. Marin, A. M. Amat, M. A. Miranda, *Appl. Catal. B* **2017**, *203*, 381-388; c) M. L. Marin, V. Lhiaubet-Vallet, L. Santos-Juanes, J. Soler, J. Gomis, A. Argues, A. M. Amat, M. A. Miranda, *Appl. Catal. B* **2011**, *103*, 48-53; d) P. Miro, A. Arques, A. M. Amat, M. L. Marin, M. A. Miranda, *Appl. Catal. B* **2013**, *140*, 412-418; e) R. Martinez-Haya, M. H. Barecka, P. Miro, M. L. Marin, M. A. Miranda, *Appl. Catal. B* **2015**, *179*, 433-438.

[11] a) D. Rehm, A. Weller, *Isr. J. Chem.* **1970**, *8*, 259-271; b) S. E. Braslavsky, *Pure Appl. Chem.* **2007**, *79*, 293-465.

[12] S. L. Murov, I. Carmichael, G. L. Hug, *Handbook of Photochemistry, 2nd ed.*, Marcel Dekker, New York, **2009**.

[13] J. W. Sease, F. G. Burton, S. L. Nickol, *J. Am. Chem. Soc.* **1968**, *90*, 2595-2598.

[14] M. Neumann, S. Füldner, B. König, K. Zeitler, *Angew. Chem. Int. Ed.* **2011**, *50*, 951-954.

[15] G. R. Buettner, *Arch. Biochem. Biophys.* **1993**, *300*, 535-543.

FULL PAPER

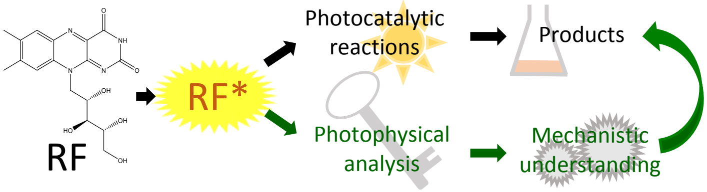

Reductive dehalogenation of organic bromides has been achieved using riboflavin (RF) as photocatalyst under visible light irradiation. The viability of the different competing processes in the time scale of the corresponding RF excited states and RF radical anion were evaluated by time-resolved techniques. Thus, the key role of the RF radical anion has been proven.

Photocatalytic mechanism*

R. Martinez-Haya, Miguel A. Miranda and M. Luisa Marin**

Page No. – Page No.

Metal-free photocatalytic reductive dehalogenation using visible-light. A time-resolved mechanistic study